Available online at www.eccomasproceedia.org
Eccomas Proceedia COMPDYN (2025) 91-104

ECCOMAS
Proceedia

COMPDYN 2025
10th ECCOMAS Thematic Conference on
Computational Methods in Structural Dynamics and Earthquake Engineering
M. Papadrakakis, M. Fragiadakis (eds.)
Rhodes Island, Greece, 15-18 June 2025

SELECTIVE MASS SCALING FOR TIMOSHENKO BEAM AND MINDLIN PLATE ELEMENTS BASED ON THE DISCRETE STRAIN GAP METHOD

Moritz Hoffmann[1], Anton Tkachuk[2], Manfred Bischoff[3] and Bastian Oesterle[1]

[1] Hamburg University of Technology, Institute for Structural Analysis
Denickestraße 17, 21073 Hamburg, Germany
e-mail: {moritz.hoffmann,bastian.oesterle}@tuhh.de

[2] Department of Engineering and Physics, Karlstad University
658 88 Karlstad, Sweden
e-mail: anton.tkachuk@kau.se

[3] University of Stuttgart, Institute for Structural Mechanics
Pfaffenwaldring 7, 70550 Stuttgart, Germany
e-mail: bischoff@ibb.uni-stuttgart.de

Abstract. *The conditional stability of explicit time integration algorithms limits the critical time step size, which depends on the highest natural frequency of the discretized problem. For shear deformable structural finite element formulations, efficiency is typically limited by the highest transverse shear frequencies. Selective mass scaling (SMS) methods aim at selectively scaling the high frequencies while preserving the important low frequency content. In particular, recent SMS concepts, which are inspired by the discrete strain gap (DSG) method [1] and, thus, are denoted as DSGSMS concepts, result in effective and accurate methods, which naturally preserve both linear and angular momentum. In this contribution, we extend previous work on DSGSMS for shear deformable element formulations [2] with respect to several aspects. First, we perform a theoretical analysis of the DSGSMS method that provides new insight into spectral properties and analytical time step estimates. Second, we extend the DSGSMS method from Timoshenko beam elements to Mindlin plate elements. Third, we test the extended concept with respect to spectral accuracy and the transient behavior in explicit time integration.*

Keywords: selective mass scaling, explicit dynamics, critical time step, Timoshenko beam elements, Mindlin plate elements, discrete strain gap method.

ISSN:2623-3347 © 2025 The Authors. Published by Eccomas Proceedia.
Peer-review under responsibility of the organizing committee of COMPDYN 2025.
doi: 10.7712/120125.12394.25480

1 INTRODUCTION

Explicit methods are very popular for highly non-linear and non-smooth transient problems including contact, inelastic material response and fracture. However, the conditional stability of explicit time integration algorithms limits the critical time step size Δt_{crit}, which depends on the highest natural angular frequency $\omega_{\max}$ of the discretized system. For the central differences method (CDM), which is used in this work, the limit of stability is defined by

$$\Delta t_{\text{crit}} = \frac{2}{\omega_{\max}}. \tag{1}$$

Mass scaling methods aim at increasing the critical time step size Δt_{crit} and thus increasing efficiency by artificially adding inertia to the system. The simplest, but most inaccurate version of mass scaling, that is conventional mass scaling (CMS), modifies the entire frequency spectrum and increases both linear and angular momentum.

In the context of SMS, it has to be distinguished between local and global strategies, see for instance [3]. In the present contribution, we restrict ourselves to local SMS methods, that is, mass scaling is performed on element level and mass matrices on system level are subsequently assembled by standard operations. Then, the general form of SMS schemes can be expressed as

$$\mathbf{m}^{\circ} = \mathbf{m} + \boldsymbol{\lambda}^{\circ}, \tag{2}$$

where $\mathbf{m}^{\circ}$, $\mathbf{m}$ and $\boldsymbol{\lambda}^{\circ}$ are the scaled element mass matrix, the initial element mass matrix and the artificial element mass matrix, respectively.

As a fundamental requirement, SMS concepts are designed such that the artificial mass matrix $\boldsymbol{\lambda}^{\circ}$ does not increase translational inertia and, thus, linear momentum is preserved. In the context of solid or solid-shell elements with translational degrees of freedom only, this is only possible if artificial inertia is added to diagonal and off-diagonal terms of the mass matrix. Due to non-diagonal artificial mass matrices, a linear system of equations has to be solved in each time step, which decreases efficiency. But, in some applications, a good compromise between accuracy and efficiency can be achieved. The SMS methods from the literature mainly differ in the design of the artificial mass matrix $\boldsymbol{\lambda}^{\circ}$. Examples for algebraic SMS methods can be given as [4, 5, 6, 7, 8, 9, 10], among others. In addition to the algebraic methods there is also a class of variational methods for selective mass scaling (VSMS), see for instance [11, 12].

However, for shear deformable structural finite element formulations with rotational degrees of freedom, to the authors' best knowledge, none of the above listed SMS methods has yet been successfully extended to the scaling of the rotational inertia. But, in the case of shear deformable structural element formulations, the rotational mass is decoupled from translational mass when a lumped mass matrix (LMM) is used. Then, it is convenient to apply CMS solely to the rotational part of the mass matrix, resulting in rotational mass scaling (RMS). Consequently, RMS preserves linear momentum and the diagonal structure of a LMM, while angular momentum is increased and the accuracy of bending frequencies is decreased. The historically important and enabling technology of RMS can be traced back to [13, 14] and still represents the state-of-the-art in explicit shell finite element analysis, as can be seen for instance from [15].

In the context of smooth discretization schemes, the concept of intrinsically selective mass scaling (ISMS) [16, 17] has been introduced. It is based on the hierarchic, intrinsically locking-free shear deformable structural formulations, see [18, 19, 20], among others, and combines the simplicity of RMS with the high accuracy of SMS. But, since ISMS builds upon hierarchic formulations, which require smooth, at least C^1-continuous discretizations, its extension to standard, C^0-continuous finite element discretizations is not directly possible. Since C^0-continuous discretization methods are still state-of-the-art in most numerical simulations of dynamic processes, the development of accurate and efficient SMS strategies for shear deformable beam, plate and shell finite element formulations is desired.

Recently, the DSGSMS method has been introduced by the group of authors in the context of Timoshenko beam elements [2] and for thin solid elements [21]. However, the present contribution focuses on shear deformable structural element formulations and extends the initial work from [2] with respect to several aspects.

The present contribution is organized as follows. Section 2 introduces the novel DSGSMS method for a two-node Timoshenko beam element. The extension of the DSGSMS method to four-node Mindlin plate elements is presented in Section 3. Inspired by the recent work of [22], both Section 2 and Section 3 provide first theoretical analyses of the DSGSMS method for structural element formulations. Next, we study the spectral properties of the DSGSMS method and investigate its accuracy in a transient problem in Section 4. In all examples, the DSGSMS method is compared to CMS and the state-of-the-art technology RMS. Section 5 summarizes our findings and gives an outlook on future developments.

2 THE DSGSMS METHOD FOR TIMOSHENKO BEAM ELEMENTS

2.1 General concept

The DSGSMS method is first introduced for a simple two-node Timoshenko beam element. As introduced in [2], the starting point for the DSG method is the removal of transverse shear locking from a two-node Timoshenko beam element. Transverse shear locking can be identified from the discrete transverse shear strain

$$\gamma \approx \gamma_{\mathrm{h}} = v_{\mathrm{h}}' + \varphi_{\mathrm{h}}, \tag{3}$$

where v_{h} and φ_{h} describe the ansatz functions for the midline displacement and for the total cross-sectional rotation of the beam. The usual element degrees of freedom are collected in the discrete displacement vector $\mathbf{d}^{\mathrm{T}} = (v_1, \varphi_1, v_2, \varphi_2)$. Furthermore, it has to be stated that $(\bullet)' = \frac{(\bullet)}{\mathrm{d}x}$ holds. For equal-order interpolation of both primary variables, the imbalance in derivatives leads to overstiff element behavior due to transverse shear locking, that is, pure bending deformation without transverse shear ($\gamma_{\mathrm{h}} = 0$) cannot be captured. For the removal of transverse shear locking from shear deformable structural elements, the DSG method from [1] can be summarized in four basic steps, which read for Timoshenko beam elements:

1. integration: $v_{\mathrm{s}}(x) = \int_0^x \gamma_{\mathrm{h}} \mathrm{d}x$
2. collocation: $v_{\mathrm{s}}^i = v_{\mathrm{s}}(x)|_{x=x_i}$
3. interpolation: $v_{\mathrm{s}}^{\mathrm{mod}}(x) = \sum_{i=1}^{n} N_i(x) v_{\mathrm{s}}^i$
4. differentiation: $\gamma^{\mathrm{mod}}(x) = (v_{\mathrm{s}}^{\mathrm{mod}}(x))'$

In the present context of Timoshenko beam elements, SMS methods have to be designed such that the highest, that is, transverse shear, frequencies are selectively scaled, while the bending frequencies remain as unaffected as possible.

The starting point for structural dynamics is d'Alembert's principle, which states that the sum of the virtual internal work, the virtual kinetic work, and the virtual external work is equal to zero:

$$\delta W = \delta W_{\mathrm{int}} + \delta W_{\mathrm{kin}} + \delta W_{\mathrm{ext}} = 0\,. \tag{4}$$

The basic idea of the DSGSMS method is to use the modified shear displacement $v_{\mathrm{s}}^{\mathrm{mod}}$ from step 3 to enrich the virtual kinetic work

$$-\delta W_{\mathrm{kin}}^{\mathrm{mod}} = \underbrace{\int_0^L \left(\delta v \rho A \ddot{v} + \delta\varphi \rho I \ddot{\varphi}\right)\,\mathrm{d}x}_{-\delta W_{\mathrm{kin}}} + \underbrace{\alpha_{\mathrm{DSG}} \int_0^L \left(\delta v_{\mathrm{s}}^{\mathrm{mod}} \rho A \ddot{v}_{\mathrm{s}}^{\mathrm{mod}}\right)\,\mathrm{d}x}_{-\delta W_{\mathrm{kin}}^{\mathrm{DSGSMS}}}\,. \tag{5}$$

The cross-sectional area, moment of inertia, density and length of the structure are denoted by A, I, ρ and L, respectively. The parameter α_{DSG} describes the scalar mass scaling parameter of the DSGSMS method.

The consistent mass matrix (CMM) of a two-node Timoshenko beam element reads

$$\mathbf{m}_{\mathrm{C}} = \int_0^l \mathbf{N}^{\mathrm{T}} \begin{bmatrix} \rho A & 0 \\ 0 & \rho I \end{bmatrix} \mathbf{N}\,\mathrm{d}x, \tag{6}$$

where $\mathbf{N}$ is the matrix of shape functions and l is the length of the element. On element level, the CMM ($\mathbf{m}_{\mathrm{C}}$) and the LMM ($\mathbf{m}_{\mathrm{L}}$, via row sum lumping) result in

$$\mathbf{m}_{\mathrm{C}} = \frac{\rho l}{3} \begin{bmatrix} A & 0 & \frac{A}{2} & 0 \\ 0 & I & 0 & \frac{I}{2} \\ \frac{A}{2} & 0 & A & 0 \\ 0 & \frac{I}{2} & 0 & I \end{bmatrix} \qquad \text{and} \qquad \mathbf{m}_{\mathrm{L}} = \frac{\rho l}{2} \begin{bmatrix} A & 0 & 0 & 0 \\ 0 & I & 0 & 0 \\ 0 & 0 & A & 0 \\ 0 & 0 & 0 & I \end{bmatrix}. \tag{7}$$

Note that CMS simply consists of multiplying $\mathbf{m}_{\mathrm{L}}$ by a scaling parameter α_{CMS}, which results in $\mathbf{m}_{\mathrm{CMS}}^{\circ}$. The RMS method solely scales the rotational inertias of $\mathbf{m}_{\mathrm{L}}$, that is, entries [2,2] and [4,4], by a factor α_{RMS}, which leads to $\mathbf{m}_{\mathrm{RMS}}^{\circ}$. As shown in [2], a naive extension of the SMS concept from Olovsson et al. [6], which was initially designed for solid elements, cannot meet the desired properties of scaling down the highest transverse shear frequency and is, thus, not further considered herein. The DSGSMS method according to Eq. (5) results in an artificial element mass matrix of the form

$$\boldsymbol{\lambda}_{\mathrm{DSGSMS}}^{\circ} = \alpha_{\mathrm{DSG}} \frac{\rho l A}{3} \begin{bmatrix} 1 & -\frac{l}{2} & -1 & -\frac{l}{2} \\ -\frac{l}{2} & \frac{l^2}{4} & \frac{l}{2} & \frac{l^2}{4} \\ -1 & \frac{l}{2} & 1 & \frac{l}{2} \\ -\frac{l}{2} & \frac{l^2}{4} & \frac{l}{2} & \frac{l^2}{4} \end{bmatrix}, \tag{8}$$

which modifies the LMM on element level by

$$\mathbf{m}_{\mathrm{DSGSMS}}^{\circ} = \mathbf{m}_{\mathrm{L}} + \boldsymbol{\lambda}_{\mathrm{DSGSMS}}^{\circ}. \tag{9}$$

2.2 Theoretical analysis

In order to test whether linear and angular momentum are modified by mass scaling, the corresponding (artificial) mass matrix can be multiplied by vectors representing unit translational and rotational/angular accelerations, that is, $\mathbf{a}_{\mathrm{t}} = \begin{bmatrix} 1 & 0 & 1 & 0 \end{bmatrix}^{\mathrm{T}}$ and $\mathbf{a}_{\mathrm{r}} = \begin{bmatrix} \frac{l}{2} & 1 & -\frac{l}{2} & 1 \end{bmatrix}^{\mathrm{T}}$, respectively. In case of the DSGSMS method, multiplying $\boldsymbol{\lambda}_{\mathrm{DSGSMS}}^{\circ}$ by $\mathbf{a}_{\mathrm{t}}$ and $\mathbf{a}_{\mathrm{r}}$ results in zero inertia forces each. Thus, DSGSMS preserves linear and angular momentum on element level. When the LMM is modified by RMS, linear momentum is preserved, while angular momentum is increased. In the case of CMS, all entries of the LMM are affected and, thus, both linear and angular momentum are manipulated which causes a large loss of accuracy.

For practical use of SMS methods, suitable time step estimates are crucial. The stability criterion from Equation (1) requires an estimation of the highest (scaled) eigenfrequency of the discretized system. It can be shown that

$$\omega_{\max} \leq \omega^{e}_{\max}, \tag{10}$$

where $\omega^{e}_{\max}$ is the highest eigenfrequency of the governing element in a finite element mesh [8]. The actual computation of $\omega^{e}_{\max}$ for each element is too expensive. This is why approximate estimators are used in practice. For SMS, however, it turns out that both the Gershgorin theorem and geometry- and material-based time step estimators are unsuitable [8]. But, for algebraic SMS methods with a fixed structure of the artificial mass matrix $\boldsymbol{\lambda}^{\circ}$, recent results from [22] show that an upper bound is defined by the ratio

$$\frac{\omega_{\max}}{\omega^{\circ}_{\max}} = \frac{\Delta t^{\circ}_{\text{crit}}}{\Delta t_{\text{crit}}} \leq \sqrt{\lambda_{\max}(\mathbf{m}^{\circ}, \mathbf{m})}, \tag{11}$$

where $\lambda_{\max}(\mathbf{m}^{\circ}, \mathbf{m})$ is the highest eigenvalue of the generalized eigenvalue problem $(\mathbf{m}^{\circ}, \mathbf{m})$. The highest unscaled frequency $\omega_{\max}$ and the corresponding critical time step size Δt_{crit} can be estimated by conventional procedures like geometry-based estimates, see for instance [23], or recent data-based estimates [24]. For the DSGSMS method and $\mathbf{m} = \mathbf{m}_{\text{L}}$, we get

$$\lambda_k(\mathbf{m}^{\circ}_{\text{DSGSMS}}, \mathbf{m}_{\text{L}}) = \begin{cases} 1 & \text{for } k = 1, 2, 3, \\ 1 + \alpha_{\text{DSG}} \frac{(Al^2+4I)}{3I} & \text{for } k = 4, \end{cases} \tag{12}$$

and consequently the time step estimate from Eq. (11) reads

$$\frac{\omega_{\max}}{\omega^{\circ}_{\max}} = \frac{\Delta t^{\circ}_{\text{crit}}}{\Delta t_{\text{crit}}} \leq \sqrt{1 + \alpha_{\text{DSG}} \frac{(Al^2 + 4I)}{3I}}. \tag{13}$$

Solving the generalized eigenvalue problem $(\mathbf{m}^{\circ}, \mathbf{m})$ for CMS and RMS yields

$$\lambda_k(\mathbf{m}^{\circ}_{\text{CMS}}, \mathbf{m}_{\text{L}}) = \alpha_{\text{CMS}} \quad \text{for } k = 1, 2, 3, 4 \tag{14}$$

and

$$\lambda_k(\mathbf{m}^{\circ}_{\text{RMS}}, \mathbf{m}_{\text{L}}) = \begin{cases} 1 & \text{for } k = 1, 2, \\ \alpha_{\text{RMS}} & \text{for } k = 3, 4, \end{cases} \tag{15}$$

respectively, which can be inserted in Eq. (11) for estimating the critical time step size.

As shown in [22], the effect of mass scaling schemes on each individual eigenfrequency can be investigated by

$$\lambda_k(\mathbf{k}, \mathbf{m}^{\circ}) = \frac{\lambda_k(\mathbf{k}, \mathbf{m})}{Q(\boldsymbol{\phi}_k)}, \qquad \text{with} \qquad Q(\boldsymbol{\phi}_k) = \frac{\boldsymbol{\phi}_k^{\text{T}} \mathbf{m}^{\circ} \boldsymbol{\phi}_k}{\boldsymbol{\phi}_k^{\text{T}} \mathbf{m} \boldsymbol{\phi}_k}, \tag{16}$$

where the $\mathbf{k}$ is the element stiffness matrix, $\boldsymbol{\phi}_k$ are the eigenvectors of the unscaled eigenvalue problem $(\mathbf{k}, \mathbf{m})$ and $Q(\boldsymbol{\phi}_k)$ denotes a Rayleigh quotient. In the following, we use two-node Timoshenko beam elements, for which we use the DSG method to remove transverse shear locking. The element stiffness matrix reads

$$\mathbf{k} = \begin{bmatrix} \frac{GA_s}{l} & -\frac{GA_s}{2} & -\frac{GA_s}{l} & -\frac{GA_s}{2} \\ -\frac{GA_s}{2} & \frac{EI}{l} + \frac{GA_s l}{4} & \frac{GA_s}{2} & -\frac{EI}{l} + \frac{GA_s l}{4} \\ -\frac{GA_s}{l} & \frac{GA_s}{2} & \frac{GA_s}{l} & \frac{GA_s}{2} \\ -\frac{GA_s}{2} & -\frac{EI}{l} + \frac{GA_s l}{4} & \frac{GA_s}{2} & \frac{EI}{l} + \frac{GA_s l}{4} \end{bmatrix}, \tag{17}$$

mode number k	mode type description	DSGSMS $Q(\boldsymbol{\phi}_k)$	CMS $Q(\boldsymbol{\phi}_k)$	RMS $Q(\boldsymbol{\phi}_k)$
1	rigid body translation	1	α_{CMS}	1
2	rigid body rotation	1	α_{CMS}	$\frac{Al^2+\alpha_{\mathrm{RMS}}2I}{Al^2+2I}$
3	bending	1	α_{CMS}	α_{RMS}
4	transverse shear	$1 + \alpha_{\mathrm{DSG}}\frac{(Al^2+4I)}{3I}$	α_{CMS}	$\frac{\alpha_{\mathrm{RMS}}Al^2+4I}{Al^2+4I}$

Table 1: Rayleigh quotients $Q(\boldsymbol{\phi}_k)$ for DSGSMS, CMS and RMS; one two-node Timoshenko beam element.

displacement	total rotations	shear strains	curvatures
v	φ_x	$\gamma_x = \frac{\partial v}{\partial x} + \varphi_y$	$\kappa_x = \frac{\partial \varphi_y}{\partial x}$
	φ_y	$\gamma_y = \frac{\partial v}{\partial y} - \varphi_x$	$\kappa_y = \frac{\partial \varphi_x}{\partial y}$
			$\kappa_{xy} = \frac{1}{2}\left(\frac{\partial \varphi_y}{\partial y} - \frac{\partial \varphi_x}{\partial x}\right)$

Table 2: Kinematic equations of the standard Mindlin plate formulation.

where GA_{s} and EI denote the shear stiffness and the bending stiffness of the cross section. Note that, in this simple case, an identical element stiffness matrix $\mathbf{k}$ could have been obtained by the assumed natural strain (ANS) method or by reduced integration. With $\mathbf{m} = \mathbf{m}_{\mathrm{L}}$, the unscaled eigenvalue problem $(\mathbf{k}, \mathbf{m})$ results in the eigenfrequencies $\lambda_1 = \lambda_2 = 0$, $\lambda_3 = \frac{4EI}{Il^2\rho}$ and $\lambda_4 = \frac{GA_s(Al^2+4I)}{AIl^2\rho}$. The corresponding eigenvectors read $\boldsymbol{\phi}_1 = \begin{bmatrix} l & 1 & 0 & 1 \end{bmatrix}^{\mathrm{T}}$ (rigid body rotation), $\boldsymbol{\phi}_2 = \begin{bmatrix} 1 & 0 & 1 & 0 \end{bmatrix}^{\mathrm{T}}$ (rigid body translation), $\boldsymbol{\phi}_3 = \begin{bmatrix} 0 & -1 & 0 & 1 \end{bmatrix}^{\mathrm{T}}$ (bending) and $\boldsymbol{\phi}_4 = \begin{bmatrix} -\frac{2I}{Al} & 1 & \frac{2I}{Al} & 1 \end{bmatrix}^{\mathrm{T}}$ (transverse shear).

With $\mathbf{k}$, $\mathbf{m}$, $\mathbf{m}^{\circ}$ and $\boldsymbol{\phi}_k$ at hand for DSGSMS, CMS and RMS, the Rayleigh quotients $Q(\boldsymbol{\phi}_k)$ are computed for the case of a two-node Timoshenko beam element and summarized in Table 1. The results show that both rigid body modes and, thus, linear and angular momentum are exactly preserved by DSGSMS. Also the bending frequency remains unaffected, while the DSGSMS method selectively scales frequency 4, which is related to transverse shear. In contrast, as expected, all frequencies are equally affected by CMS, which results in unphysical behavior and limits wide application. From the last column it can be seen that RMS preserves the translational rigid body mode and the corresponding frequency. Thus, RMS is able to preserve linear momentum. But, the modification of frequencies 2 and 3, which are related to rigid body rotation and bending, comes along with a loss of accuracy. Note that the largest Rayleigh quotient is associated with the bending frequency rather than with the shear frequency.

3 THE DSGSMS METHOD FOR MINDLIN PLATE ELEMENTS

3.1 General concept

Next, we focus on the Mindlin plate model assuming linearized kinematics and linear elastic, isotropic and homogeneous material behavior, as presented in [25]. The kinematic variables and the stress resultants are defined in Fig. 1, with a and b denoting the plate's length in x- and y-direction, respectively. The kinematic equations for the standard Mindlin plate formulation with v, φ_x and φ_y as primary variables are shown in Table 2. The constitutive equation connects the

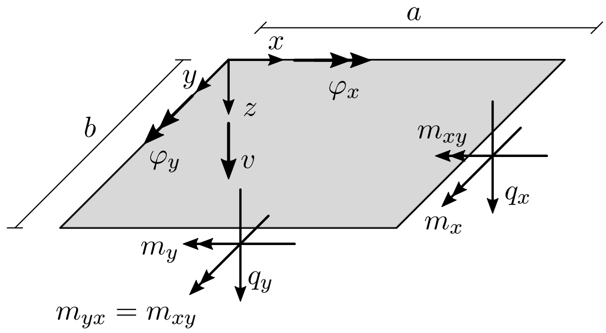

Figure 1: Kinematic variables and stress resultants (bending moments m_x and m_y, twisting moment m_{xy} and transverse shear forces q_x and q_y) of the Mindlin plate model.

stress resultants from Fig. 1 to the strain components from Table 2 via the material matrix $\mathbf{C}$

$$\underbrace{\begin{bmatrix} m_x \\ m_y \\ m_{xy} \\ q_x \\ q_y \end{bmatrix}}_{\boldsymbol{\sigma}} = \underbrace{\begin{bmatrix} D & \nu D & 0 & 0 & 0 \\ \nu D & D & 0 & 0 & 0 \\ 0 & 0 & \frac{D}{2}(1-\nu) & 0 & 0 \\ 0 & 0 & 0 & Gd & 0 \\ 0 & 0 & 0 & 0 & Gd \end{bmatrix}}_{\mathbf{C}} \underbrace{\begin{bmatrix} \kappa_x \\ \kappa_y \\ 2\kappa_{xy} \\ \gamma_x \\ \gamma_y \end{bmatrix}}_{\boldsymbol{\varepsilon}}, \tag{18}$$

with $D = \frac{Ed^3}{12(1-\nu^2)}$ being the plate modulus, which is a function of Young's modulus E, Poisson's ratio ν and the plate's thickness d. The parameter G denotes the shear modulus.

The standard Mindlin formulation suffers from transverse shear locking, as can be seen from the kinematic equations for the shear strains γ_x and γ_x in Table 2. Again, like for the Timoshenko beam, any equal order interpolation of the primary variables results in parasitic transverse shear strains and overstiff behavior. For removing transverse shear locking from Mindlin plate elements the DSG method from [1] can be summarized as:

1. integration: $v_{\mathrm{s}_x}(x,y) = \int_0^x \gamma_x^{\mathrm{h}}(x,y)\mathrm{d}x$ and $v_{\mathrm{s}_y}(x,y) = \int_0^y \gamma_y^{\mathrm{h}}(x,y)\mathrm{d}y$
2. collocation: $v_{\mathrm{s}_x}^i = v_{\mathrm{s}_x}(x,y)|_{x=x_i,y=y_i}$ and $v_{\mathrm{s}_y}^i = v_{\mathrm{s}_y}(x,y)|_{x=x_i,y=y_i}$
3. interpolation: $v_{\mathrm{s}_x}^{\mathrm{mod}}(x,y) = \sum_{i=1}^n N_i(x,y)v_{\mathrm{s}_x}^i$ and $v_{\mathrm{s}_y}^{\mathrm{mod}}(x,y) = \sum_{i=1}^n N_i(x,y)v_{\mathrm{s}_y}^i$
4. differentiation: $\gamma_x^{\mathrm{mod}}(x,y) = \frac{\partial(v_{\mathrm{s}_x}^{\mathrm{mod}}(x,y))}{\partial x}$ and $\gamma_y^{\mathrm{mod}}(x,y) = \frac{\partial(v_{\mathrm{s}_y}^{\mathrm{mod}}(x,y))}{\partial y}$

For Mindlin plate elements, the DSGSMS method enriches the virtual kinetic work with the modified shear displacements $v_{\mathrm{s}_x}^{\mathrm{mod}}$ and $v_{\mathrm{s}_y}^{\mathrm{mod}}$ from step 3:

$$-\delta W_{\mathrm{kin}}^{\mathrm{mod}} = \underbrace{\int_\Omega \delta\mathbf{u}^{\mathrm{T}}\boldsymbol{\rho}\ddot{\mathbf{u}}\,\mathrm{d}\Omega}_{-\delta W_{\mathrm{kin}}} + \underbrace{\alpha_{\mathrm{DSG}}\int_\Omega \left(\delta v_{\mathrm{s}_x}^{\mathrm{mod}}\rho d\ddot{v}_{\mathrm{s}_x}^{\mathrm{mod}} + \delta v_{\mathrm{s}_y}^{\mathrm{mod}}\rho d\ddot{v}_{\mathrm{s}_y}^{\mathrm{mod}}\right)\,\mathrm{d}\Omega}_{-\delta W_{\mathrm{kin}}^{\mathrm{DSGSMS}}}. \tag{19}$$

In the present version, both contributions from $-\delta W_{\mathrm{kin}}^{\mathrm{DSGSMS}}$ are scaled by the same parameter α_{DSG}. But, in general, it is possible to define two independent scaling parameters. The consistent element mass matrix $\mathbf{m}_{\mathrm{C}}$ is constructed by the density matrix $\boldsymbol{\rho}$ and the matrix of shape functions $\mathbf{N}$, which is defined w.r.t. the displacement v and the total fiber rotations φ_x and φ_y:

$$\mathbf{m}_{\mathrm{C}} = \int_{\Omega_{\mathrm{ele}}} \mathbf{N}^{\mathrm{T}} \boldsymbol{\rho} \mathbf{N} \,\mathrm{d}\Omega \tag{20}$$

with

$$\boldsymbol{\rho} = \begin{bmatrix} \rho d & 0 & 0 \\ 0 & \frac{\rho d^3}{12} & 0 \\ 0 & 0 & \frac{\rho d^3}{12} \end{bmatrix}. \tag{21}$$

As for the Timoshenko beam element, The DSGSMS method according to Eq. (19) results in an artificial element mass matrix $\boldsymbol{\lambda}^{\circ}_{\mathrm{DSGSMS}}$ for a Mindlin plate element. Again, modification of the LMM is performed on element level in the form of Eq. (9). For the sake of brevity, we refrain from showing the expressions for $\mathbf{m}_{\mathrm{C}}$, $\mathbf{m}_{\mathrm{L}}$, $\boldsymbol{\lambda}^{\circ}_{\mathrm{DSGSMS}}$ and $\mathbf{m}^{\circ}_{\mathrm{DSGSMS}}$ in detail. The same consideration holds for the stiffness matrix $\mathbf{k}$. Again, we use the DSG method, as described in this section, to remove transverse shear locking from a four-node Mindlin plate element.

3.2 Theoretical analysis

According to Eq. (11), the highest eigenvalue $\lambda_{\max}(\mathbf{m}^{\circ}, \mathbf{m})$ of the generalized eigenvalue problem $(\mathbf{m}^{\circ}, \mathbf{m})$ is essential for estimating the critical time step size. For a rectangular four-node Mindlin plate element, the DSGSMS method yields

$$\lambda_k(\mathbf{m}^{\circ}_{\mathrm{DSGSMS}}, \mathbf{m}_{\mathrm{L}}) = \begin{cases} 1 & \text{for } k = 1, .., 8, \\ 1 + \alpha_{\mathrm{DSG}} \frac{(6a^2+6b^2+4d^2)-\sqrt{(9a^4-18a^2b^2+9b^2+4d^4)}}{3d^2} & \text{for } k = 9, \\ 1 + \alpha_{\mathrm{DSG}} \frac{(6a^2+6b^2+4d^2)+\sqrt{(9a^4-18a^2b^2+9b^2+4d^4)}}{3d^2} & \text{for } k = 10, \\ 1 + \alpha_{\mathrm{DSG}} \frac{(4d^2+12b^2)}{3d^2} & \text{for } k = 11, \\ 1 + \alpha_{\mathrm{DSG}} \frac{(4d^2+12a^2)}{3d^2} & \text{for } k = 12. \end{cases} \tag{22}$$

Solving the generalized eigenvalue problem $(\mathbf{m}^{\circ}, \mathbf{m})$ for CMS and RMS results in

$$\lambda_k(\mathbf{m}^{\circ}_{\mathrm{CMS}}, \mathbf{m}_{\mathrm{L}}) = \alpha_{\mathrm{CMS}} \quad \text{for } k = 1, .., 12 \tag{23}$$

and

$$\lambda_k(\mathbf{m}^{\circ}_{\mathrm{RMS}}, \mathbf{m}_{\mathrm{L}}) = \begin{cases} 1 & \text{for } k = 1, 2, 3, 4, \\ \alpha_{\mathrm{RMS}} & \text{for } k = 5, .., 12, \end{cases} \tag{24}$$

respectively.

Unfortunately, for the Mindlin plate element, we were not able to solve the eigenvalue problem $\lambda_k(\mathbf{k}, \mathbf{m}^{\circ})$ symbolically. Thus, we also did not obtain analytical expressions for the Rayleigh quotients $Q(\boldsymbol{\phi}_k)$, as we were able to obtain for the Timoshenko beam element. But, analytical expressions for upper bounds for the critical time step sizes exist with Eq. (11) and Eqs. (22), (23) and (24), what will be shown in Section 4. Nevertheless, like for the Timoshenko beam element, Eqs. (22), (23) and (24) indicate that the DSGSMS method is more accurate than RMS and CMS, since for DSGSMS the highest number of eigenvalues remains unaffected.

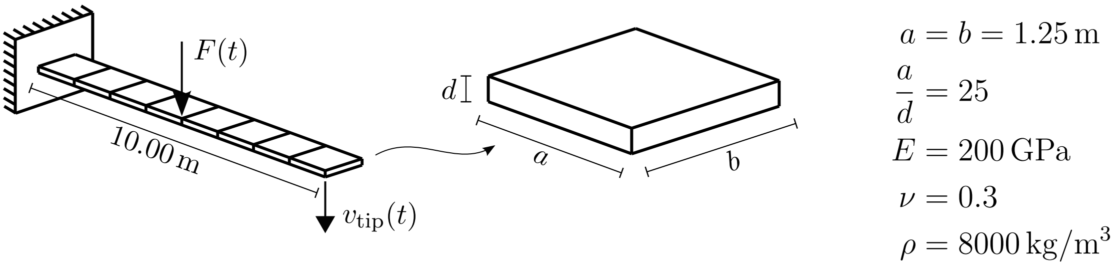

Figure 2: Eccentrically loaded cantilever, problem setup.

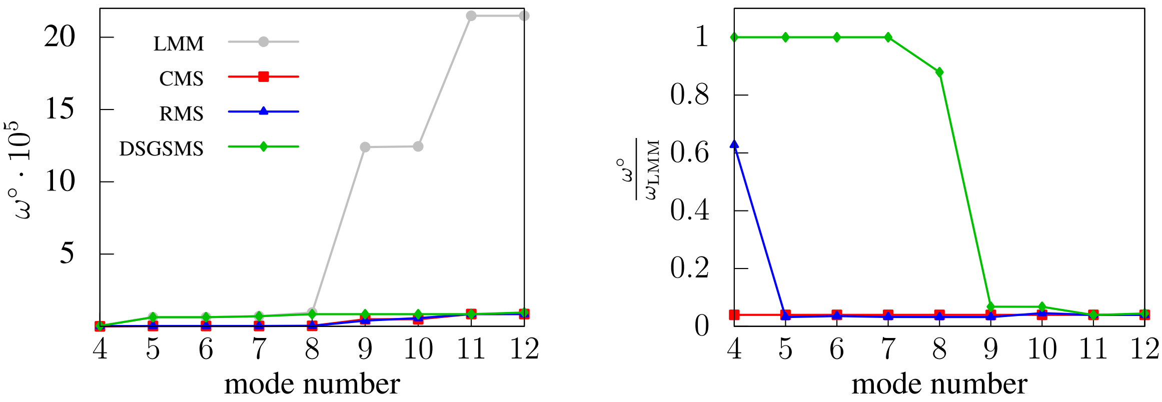

Figure 3: Frequency spectra of a four-node Mindlin plate element, left: eigenfrequency spectra of different mass scaling methods in comparison (without the three rigid body modes), right: ratio of scaled to unscaled eigenfrequencies.

4 NUMERICAL STUDIES

In this section, we investigate the problem of a cantilever plate, as shown in Figure 2. The cantilever is discretized with eight four-node Mindlin elements with in-plane dimensions $a = b = 1.25\,\mathrm{m}$ and thickness $d = 0.05\,\mathrm{m}$, which results in a high element aspect ratio of $\frac{a}{d} = 25$. Further geometry and material data are given in Figure 2. Transverse shear locking is removed by the DSG method, as described in Section 3. At the clamped edge, all degrees of freedom are fixed. In mid-length, the cantilever is eccentrically loaded by a time-dependent load $F(0 \leq t \leq 0.05\,\mathrm{s}) = 3\,\mathrm{kN}$, which will play a role in the transient solution of the problem.

But, first, we study the spectral accuracy of one four-node Mindlin element with a fixed aspect ratio of $\frac{a}{d} = 25$ and different mass scaling methods, that is, CMS, RMS and DSGSMS. No boundary are assigned. The corresponding mass scaling parameters are chosen as $\alpha_{\mathrm{CMS}} = 635$, $\alpha_{\mathrm{RMS}} = 970$ and $\alpha_{\mathrm{DSG}} = 0.26$. This particular choice is motivated by the scaling limit for the DSGSMS method in the cantilever problem setup with eight elements, which will be discussed later. For this one-element problem, the highest natural angular eigenfrequency $\omega_{\max}$ is scaled by 95.5% compared to LMM. For this high scaling level, it is remarkable that frequency number eight seems to be slightly modified for DSGSMS, although Eq. (22) indicates, that the first eight frequencies are not affected. In fact, the scaling parameter α_{DSG} is slightly too large for this one-element test, what causes a scaling of eigenfrequencies 9-12 below the highest, absolutely unmodified bending frequency, that is, initial eigenfrequency number eight. This means that there is only a change in the order of the eigenvalues due to excessive mass scaling. This change can be tracked by computing the eigenfrequencies numerically via Rayleigh

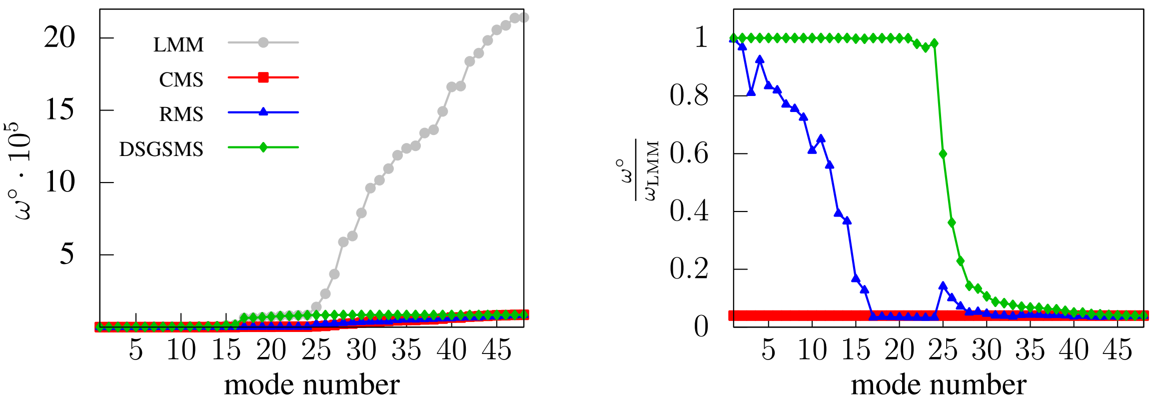

Figure 4: Frequency spectra of the cantilever, left: eigenfrequency spectra of different mass scaling methods in comparison, right: ratio of scaled to unscaled eigenfrequencies.

quotients, which is, for the sake of brevity, not shown in more detail. As expected, CMS scales all frequencies by the same ratio, leading to inaccurate results. But, for this setup, also RMS shows low accuracy. Only frequency number four is not as much affected as the others. This again can be shown by numerical evaluation of the Rayleigh quotients, but cannot be seen from Eq. (24). A similar behavior can be observed for the Timoshenko beam element, but, in this case, analytically, as shown in Eq. (15) and Table 1.

Next, we study the spectral accuracy of the cantilever plate, discretized with eight Mindlin plate elements, as shown in Figure 2. The element aspect ratio and the scaling factors remain identical to the previous investigation, but the maximum reduction of the highest frequency is slightly increased to 96%. The spectra for LMM and the different scaled mass matrices are shown in the left of Figure 4, the ratio of scaled to unscaled eigenfrequencies is shown on the right. Again, the results underline the high accuracy of DSGSMS. With mesh refinement, the lowest frequencies obtained by RMS improved compared to the previous test with one element, but still severe loss of accuracy in the first half of the spectrum is visible. As expected, applying CMS to the whole structure scales the whole spectrum and provides the lowest accuracy of the three investigated mass scaling concepts.

The effect of the spectral accuracy on the transient behavior within explicit time integration using the central differences scheme is investigated next. Figure 5 shows the eccentric cantilever's tip displacement $v_{\text{tip}}(t)$ over a simulation time of $3\,\text{s}$ on the left and a detailed view on the right. The eccentric load in mid-length of the cantilever is applied for the first $0.05\,\text{s}$, that is, $F(0 \leq t \leq 0.05\,\text{s}) = 3\,\text{kN}$. The number of time steps used for LMM, DSGSMS, RMS, CMS is 321306, 12738, 12708, 12751, respectively. The results for DSGSMS are practically identical to the unscaled solution obtained by LMM, but require only 4% of the time steps. The results demonstrate the superior accuracy of DSGSMS over RMS, also in the transient case. Of course, the accuracy of all mass scaling concepts depends on the range of relevant frequencies, which is problem-dependent.

Last, as shown in [22], we motivate the choice of $\alpha_{\text{DSG}} = 0.26$ and validate the theoretical results from Section 3.2. Figure 6 (left) shows that the estimate of the highest eigenfrequency from Eq. (22) is very sharp, until the maximum value is reached, due to the highly selective nature of DSGSMS. For the RMS method, the upper bound from Eq. (24) is not as sharp as for DSGSMS. Further detailed investigations on these interesting properties are planned in future.

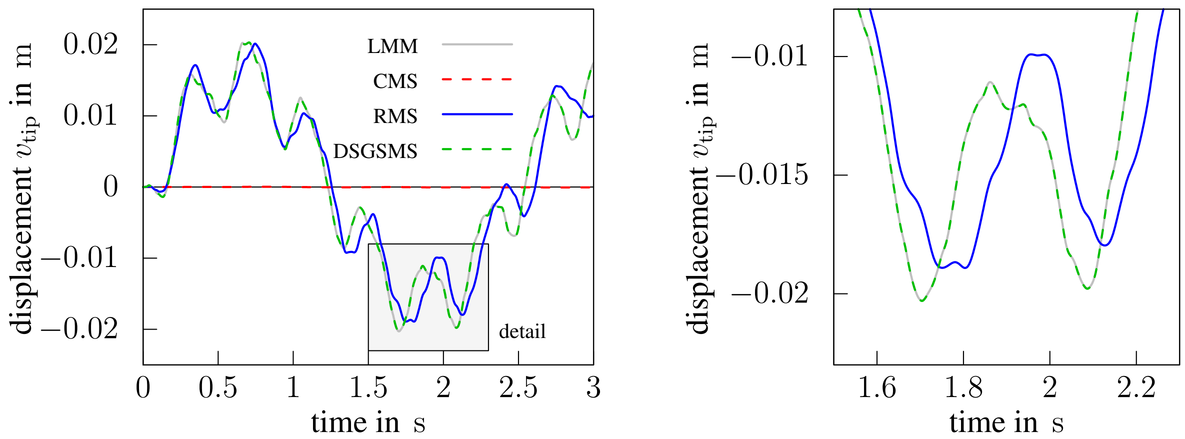

Figure 5: Transient analysis of the cantilever for $F(0 \leq t \leq 0.05\,\mathrm{s}) = 3\,\mathrm{kN}$, and a reduction of the maximum eigenfrequency by 96% compared to LMM, left: full computation time, right: detail.

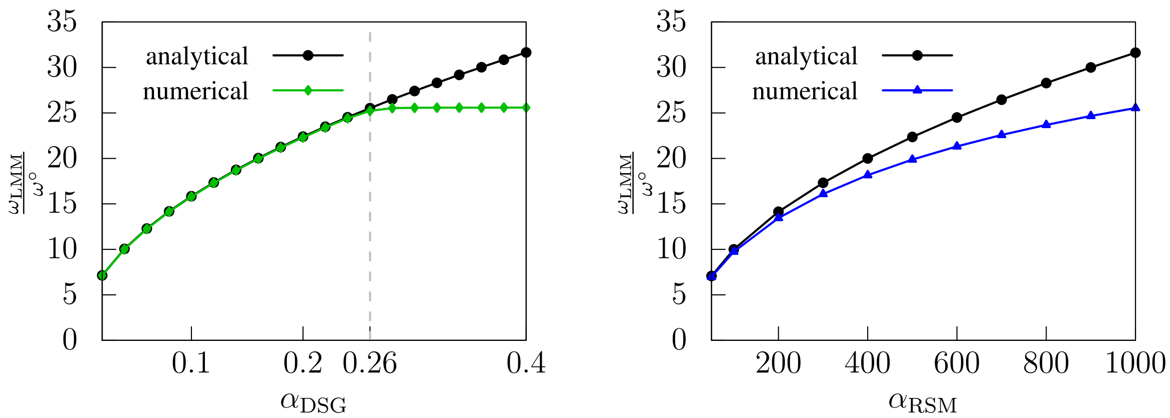

Figure 6: Cantilever, ratio of unscaled to scaled eigenfrequencies over the scaling parameters α_{DSG} (left) and α_{RMS} (right).

5 CONCLUSIONS AND OUTLOOK

In this paper, we extended the DSGSMS method from Timoshenko beam elements to Mindlin plate elements. For both beam and plate elements, we performed a theoretical analysis of the DSGSMS method in comparison to CMS and RMS, the state-of-the-art technology for explicit dynamics using structural element formulations, especially shell elements. The theoretical results gave new insight in the accuracy of the presented mass scaling concepts and were validated in numerical experiments. The presented numerical results for spectral problems and transient analyses indicate that DSGSMS is a promising method for efficient and accurate explicit dynamics of thin-walled structures.

In future work, several aspects need to be addressed. First, the DSGSMS concept needs to extended to shell elements. In this context, the development of an isotropic DSGSMS method, as developed for solid elements in [21], may be crucial for efficient simulation of non-linear problems involving large rotations. Furthermore, conditioning and fill-in of scaled mass matrices and their influence on the efficiency of iterative solvers need to be investigated. This is particularly relevant for assessing the actual speed-up by DSGSMS in larger problems, while keeping the error below a certain threshold.

ACKNOWLEDGEMENTS

This project is supported by the Deutsche Forschungsgemeinschaft (DFG, German Research Foundation) under Grant OE 728/3-1 – 512271632. This support is gratefully acknowledged. We thank Carola Zeh for her investigations in the early phase of this project.

REFERENCES

[1] Bletzinger, K.-U., Bischoff, M. and Ramm, E., A unified approach for shear-locking-free triangular and rectangular shell finite elements, *Computers & Structures*, **75**, 32–334, 2000.

[2] Oesterle, B., Tkachuk, A., Bischoff, M., Finite element technology-based selective mass scaling for shear-deformable structural element formulations. *Eccomas Proceedia COMPDYN (2023)*, 1965–1973, 2023.

[3] Tkachuk, A. and Bischoff, M., Local and global strategies for optimal selective mass scaling, *Computational Mechanics*, **53**, 1197–1207, 2014.

[4] Macek R. W. and und Aubert, B. H., A mass penalty technique to control the critical time increment in explicit dynamic finite element analyses. *Earthquake Engineering & Structural Dynamics*, **24**, 1315–1331, 1995.

[5] Olovsson, L., Unosson, M. and Simonsson, K., Selective mass scaling for thin walled structures modeled with tri-linear solid elements. *Computational Mechanics*, **34**, 134–136, 2004.

[6] Olovsson, L., Simonsson, K. and Unosson, M., Selective mass scaling for explicit finite element analyses. *International Journal for Numerical Methods in Engineering*, **63** , 1436–1445, 2005.

[7] Askes, H., Nguyen, D. C. D. and Tyas, A. Increasing the critical time step: micro-inertia, inertia penalties and mass scaling. *Computational Mechanics*, **47** , 657–667, 2011.

[8] Cocchetti, G. , Pagani, M. and Perego, U. Selective mass scaling and critical time-step estimate for explicit dynamics analyses with solid-shell elements.*Computers & Structures*, **127**, 39–52, 2013.

[9] Mattern, S., Schmied, C. and Schweizerhof, K., Highly efficient solid and solid-shell finite elements with mixed strain–displacement assumptions specifically set up for explicit dynamic simulations using symbolic programming, *Computers & Structures*, **154**, 210–225, 2015.

[10] González, J. A. and Park, K. C., Large-step explicit time integration via mass matrix tailoring, *International Journal for Numerical Methods in Engineering*, **121**, 1647–1664, 2020.

[11] Tkachuk, A. and Bischoff, M., Variational methods for selective mass scaling, *Computational Mechanics*, **52**, 563–570, 2013.

[12] Stoter, S. K. F., Nguyen,T.-H., Hiemstra, R. R. and Schillinger, D. Variationally consistent mass scaling for explicit time-integration schemes of lower- and higher-order finite element methods. *Computer Methods in Applied Mechanics and Engineering*, **399**, 115310, 2022.

[13] Hughes, T. J. R., Cohen, M. and Haroun, M., Reduced and selective integration techniques in the finite element analysis of plates. *Nuclear Engineering and Design*, **46**, 203–222, 1978.

[14] Belytschko, T. and Mindle, W. L., Flexural wave propagation behavior of lumped mass approximations, *Computers & Structures*, **12**, 805–812, 1980.

[15] Hartmann, S. and Benson, D., Mass scaling and critical time step estimates for isogeometric analysis, *International Journal for Numerical Methods in Engineering*, **102**, 671–687, 2015.

[16] Oesterle, B., Trippmacher, J., Tkachuk, A. and M. Bischoff, M., Intrinsically Selective Mass Scaling With Hierarchic Structural Element Formulations, *Book of Extended Abstracts of the 6th ECCOMAS Young Investigators Conference, 7th-9th July 2021, Valencia, Spain*, 99–108, 2021.

[17] Krauß, L.-M., Thierer, R., Bischoff, M. and Oesterle, B. Intrinsically selective mass scaling with hierarchic plate formulations. *Computer Methods in Applied Mechanics and Engineering*, **432**, 117430, 2024.

[18] Oesterle, B., Ramm, E. and Bischoff, M.: A shear deformable, rotation-free isogeometric shell formulation. *Computer Methods in Applied Mechanics and Engineering*, **307**, 235–255, 2016.

[19] Oesterle, B., Bieber, S., Sachse, R., Ramm, E. and Bischoff, M.: Intrinsically locking-free formulations for isogeometric beam, plate and shell analysis. *PAMM*, **18**, e201800399, 2018.

[20] Oesterle B. *Intrinsisch lockingfreie Schalenformulierungen*. PhD Thesis, Stuttgart: Institut für Baustatik und Baudynamik, Universität Stuttgart, 2018.

[21] Hoffmann, M., Tkachuk, A., Bischoff, M., Oesterle, B., Finite element technology-based selective mass scaling for explicit dynamic analyses of thin-walled structures using solid elements. *Eccomas Proceedia COMPDYN (2023)*, 1974–1982, 2023.

[22] Voet, Y., Sande, E. and Buffa, A., A theoretical analysis of mass scaling techniques, *arXiv*, 2410.23816, 2024.

[23] Benson, D. J.: Explicit Finite Element Methods for Large Deformation Problems in Solid Mechanics. In: *Encyclopedia of Computational Mechanics*. John Wiley & Sons, Ltd, 2007.

[24] Willmann, T., Schilling, M. and Bischoff, M., Data-Based Estimation of Critical Time Steps for Explicit Time Integration, *International Journal for Numerical Methods in Engineering*, **126**, e7666, 2025.

[25] Mindlin, R. D., Influence of Rotatory Inertia and Shear on Flexural Motions of Isotropic, Elastic Plates, *Journal of Applied Mechanics*, **18**, 31–38, 1951.